ACS APPLIED MATERIALS & INTERFACES

Research Article

www.acsami.org

Local Electronic Structures and Electrical Characteristics of Well-Controlled Nitrogen-Doped ZnO Thin Films Prepared by Remote Plasma In situ Atomic Layer Doping

Jui-Fen Chien,[†] Ching-Hsiang Chen,[‡] Jing-Jong Shyue,[†,§] and Miin-Jang Chen*[,†,⊥,∥]

[†]Department of Materials Science and Engineering and [⊥]Center for Emerging Material and Advanced Devices, National Taiwan University, Taipei 10617, Taiwan, Republic of China

[‡]Protrustech Corporation Limited, 3F.-1, No.293, Sec. 3, Dongmen Rd, East District, Tainan, 701, Taiwan

[§]Research Center for Applied Sciences, Academia Sinica, 128 Sec. 2, Academia Rd., Nankang, Taipei 11529, Taiwan

[∥]National Nano Device Laboratories, Hsinchu 30078, Taiwan

ABSTRACT: Nitrogen-doped ZnO (ZnO:N) films were prepared by remote plasma in situ atomic layer doping. X-ray photoelectron and absorption near-edge spectroscopies reveal the presence of Zn−N bond and a decrease in strength of the O 2p hybridized with Zn 4s states, which are consistent with the decrease of electron concentration in ZnO:N films with increasing nitrogen content and indicate the formation of acceptor states by occupation of oxygen sites with nitrogen. Linear dependence between the nitrogen content and the atomic layer doping percentage indicates the electrical properties and local electronic structures can be precisely controlled using this atomic layer doping technique.

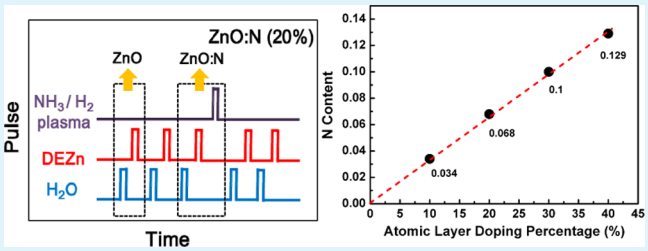

KEYWORDS: *in situ atomic layer doping, remote plasma, zinc oxide, X-ray absorption near edge spectroscopy, X-ray photoelectron spectroscopy, atomic layer deposition*

INTRODUCTION

Zinc oxide (ZnO) has attracted great attention as an ultraviolet (UV) material because of its large exciton binding energy (60 meV) and wide direct bandgap (3.37 eV).[1−6] ZnO has been used in a variety of applications, such as UV light-emitting diodes (LEDs)[2,3] and transparent thin film transistors (TFTs).[4,5] However, undoped ZnO exhibits intrinsic n-type conductivity due to various nonstoichiometric defects, for example, Zn interstitials and O vacancies.[7] It has been reported that p-type conductivity can be achieved by doping with group-V elements (N, P, and As) as substituting for O sites in ZnO.[8−10] Since the bond length of Zn−O is significantly shorter than that of Zn−P and Zn−As, phosphorus and arsenic tend to form antisite deep-level states (P_{Zn} and As_{Zn}) in ZnO.[10] Nitrogen is considered as a promising p-type dopant because the ionic radius of N is close to O, which leads to facile substitution. Thus nitrogen-doped ZnO (ZnO:N) thin films have been applied in ZnO homojunction LEDs[11,12] and active channel layers in TFTs.[13] As the ZnO thin films were prepared by low-temperature processes, the film structure would be amorphous or low-level crystalline. Because there are no grain boundaries in amorphous ZnO, the film is preferred as a channel material in TFTs.[14−16] Even in the absence of grain boundaries, electron mobility at the band edges in a disordered system is reduced by random atomic arrangements due to the loss of lattice periodicity.[17] On the other hand, for the ZnO thin films prepared by high-temperature processes, electron mobility in crystalline ZnO is limited by defects, such as oxygen vacancies, dislocations, and impurities, at the grain boundaries. Therefore, the details of the local electronic structures of the ZnO thin films are of great interest for understanding their electrical properties.

Many techniques have been developed to prepare ZnO thin films doped with group-V elements, including metal−organic chemical vapor deposition,[18,19] molecular beam epitaxy,[11,20] pulse laser deposition,[21,22] and sputtering.[23,24] Atomic layer deposition (ALD) is an alternative thin-film deposition method for preparing high-quality ZnO thin films due to the self-limiting characteristics.[25−28] As compared with other techniques, the advantages of ALD include accurate thickness and composition control, excellent step coverage and conformality, high uniformity over a large area, low defect density, good reproducibility, and low deposition temperatures. In addition, because of layer-by-layer (or "digital") growth, ALD has the in situ doping capability of achieving high dopant concentration while maintaining atomic level control of the doping process. Recently, atomic layer doping technique by stacking of multiple δ layers was demonstrated to achieve high phosphorus concentrations and low resistivity in germanium.[29] In this study, well-controlled ZnO:N thin films were prepared by in

Received: March 29, 2012
Accepted: June 11, 2012
Published: June 11, 2012

situ atomic layer doping based on the ALD technique. The nitrogen radicals were generated in remote NH_3/H_2 plasma and in situ incorporated into ZnO during the film growth. The benefit of remote plasma is the minimization of plasma-induced damages due to no direct wafer exposure to the plasma. The correlation between the local electronic structures and the electrical properties of the ZnO:N films was investigated using X-ray photoelectron spectroscopy (XPS), X-ray absorption spectroscopy (XAS) and Hall effect measurement. In XAS, X-ray absorption near edge spectroscopy (XANES) indicates the fingerprint of the oxidation state and site symmetry of the element. The high degree of sensitivity to the coordination environment of the absorber atom in XANES results from the perturbation of the wave function of the ejected photoelectron caused by multiple scattering from the surrounding atoms.[30,31] Therefore, XANES at O *K*-edge, N *K*-edge, and Zn L_{III}-edge was employed to analyze the variations in absorption edge of the ZnO:N thin films in this work.

EXPERIMENTAL SECTION

ZnO:N thin films of thickness about 170 nm were deposited on (0002)-oriented sapphire substrates at a low temperature of 180 °C using ALD (Fiji F202, Cambridge Nanotech). Diethylzinc (DEZn, Zn $(C_2H_5)_2$), H_2O vapor, and NH_3 were utilized as the precursors for zinc, oxygen, and nitrogen, respectively. The process was composed of two kinds of ALD cycles, the first contained the following sequence: DEZn → Ar purge → H_2O → Ar purge for the deposition of ZnO, and the second contained DEZn → Ar purge → remote NH_3/H_2 plasma → Ar purge → H_2O → Ar purge for the in situ atomic layer doping of nitrogen into ZnO films. The pressure in the ALD chamber was approximately 3×10^{-1} Torr. The remote NH_3/H_2 plasma was generated by a radio frequency (RF) coil under a RF power of 300 W. Multiple atomic doped layers were introduced into the ZnO films and the ALD cycles for in situ atomic layer doping were uniformly distributed in a total of 1000 ALD cycles. The atomic layer doping percentage can be precisely controlled by the number of atomic doped layers and their separation in the films. For example, one ALD cycle for atomic layer doping was performed every 9 ZnO ALD cycles for preparing the nominal ZnO:N(10%) film, i.e., the ZnO:N film with nitrogen atomic layer doping percentage of 10%. The nitrogen atomic layer doping percentages in the ZnO:N films, from 10 to 40%, can be precisely controlled by the number of the ALD cycles for nitrogen in situ atomic layer doping. Afterward, the ZnO:N thin films were treated by RTA at 1000 °C in oxygen atmosphere for 5 min in order to improve the uniformity of dopant distribution and crystalline quality.

The crystalline structure and electrical properties of the ZnO:N thin films were characterized by X-ray diffraction (XRD) and Hall effect measurement. The XRD patterns were recorded by the X-ray diffractometer (X'Pert PRO, PANalytical) in $\theta-2\theta$ mode with Cu $K\alpha$ radiation. The carrier concentration, mobility, and conductivity type of the films were measured by Ecopia HMS-3000 Hall-effect measurement system in the van der Pauw configuration at room temperature. The XPS technique (PHI 5000 VersaProbe, ULVAC-PHI) was used to investigate the chemical state of N element and determine the N content in the ZnO:N films. The binding energy was referenced with respect to the Au $4f_{7/2}$ line at 84 eV. Soft XAS measurements were carried out at the BL20A1 station of the National Synchrotron Radiation Research Center (NSRRC), in Hsinchu, Taiwan. The energy and current of the storage ring were 1.5 GeV and 300 mA, respectively. Those measurements were performed in the total electron yield mode for O *K*-edge, N *K*-edge, and Zn L_{III}-edge, in an ultrahigh-vacuum (UHV) chamber, with a base pressure of 1×10^{-10} Torr. Photoluminescence (PL) spectroscopy was conducted using a pulsed Q-switched diode-pumped solid-state laser (Advanced Optowave Corporation, λ = 266 nm, repetition rate = 15 kHz).

RESULTS AND DISCUSSION

Figure 1 shows the variation of the N content in the ZnO:N films with the nitrogen atomic layer doping percentage,

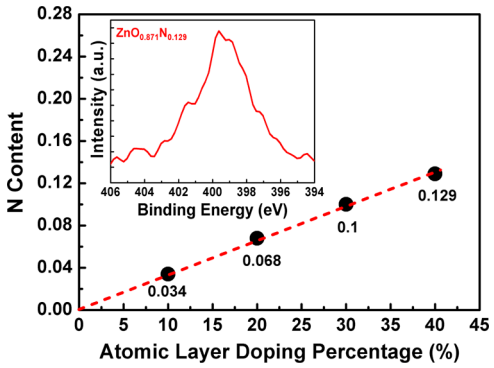

Figure 1. N content as a function of the nitrogen atomic layer doping percentage in ZnO:N thin films. Inset shows the XPS spectrum of $ZnO_{0.871}N_{0.129}$ films.

identified by quantitative analysis of the XPS spectra. The insert shows the XPS spectrum of the N 1s peak at ~399.2 eV associated with the Zn−N bond, indicating the substitution of N for O in the ZnO:N films.[14,34] The $ZnO_{0.871}N_{0.129}$ as indicated in the inset of Figure 1 indicates that the actual atomic compositions of O and N are 87.1 and 12.9%, which corresponds to the nominal ZnO:N(40%) thin film with the nitrogen atomic layer doping percentage of 40%. The smaller atomic composition of N in the ZnO:N films than the nitrogen atomic layer doping percentage can be attributed to the partial incorporation of nitrogen, not self-limiting, in each ALD cycle for in situ atomic layer doping, because the introduction of remote NH_3/H_2 plasma was followed by the oxygen precursor (H_2O vapor) and the Zn−O bond is stronger than the Zn−N bond. It is seen that an N content in the ZnO:N films increases linearly with the nitrogen atomic layer doping percentage. This linearity indicates that the N content can be precisely controlled by the number of atomic doped layers, clearly indicating that the in situ atomic layer doping technique is a well-controlled process. It should be noted that the N content as high as 12.9% can be achieved using this in situ atomic layer doping technique.

Figure 2 shows that XRD patterns of the pure ZnO and ZnO:N thin films with different N contents. The pure ZnO and ZnO:N thin films have dominant *c*-axis orientation with (0002)

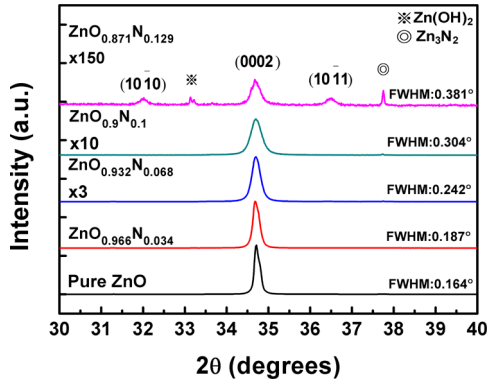

Figure 2. XRD patterns of the pure ZnO and ZnO:N thin films.

dx.doi.org/10.1021/am300551y | ACS Appl. Mater. Interfaces 2012, 4, 3471−3475

face reflection at ~34.7°, namely, the *c*-axis of the grains is perpendicular to the substrate surface. The intensity and full-width at half-maximum (FWHM) of XRD (0002) peak significantly decrease and broaden with the increase of the N content. A slight shift of the (0002) peak toward the low-angle side reveals the grains undergo a tensile strain along the *c*-axis due to the partial substitution of larger N atoms (r_N = 0.75 Å) for smaller O atoms (r_O = 0.65 Å). As for the $ZnO_{0.871}N_{0.129}$ thin films, two weak ZnO ($10\bar{1}0$) and ($10\bar{1}1$) peaks together with those belonging to $Zn(OH)_2$ and Zn_3N_2 were observed,[32,33] which can be attributed to the distortion of ZnO lattice due to the incorporation of a large amount of nitrogen.

The O *K*-edge XANES spectra in total electron yield mode of the pure ZnO and ZnO:N thin films with different N contents, along with that of the sapphire substrate, are shown in Figure 3(a). The total electron yield mode is surface sensitive while the fluorescence yield mode is suitable for bulk study. The ligand *K*-edge XAS is very sensitive to the chemical environment around the ligand element and the electronic

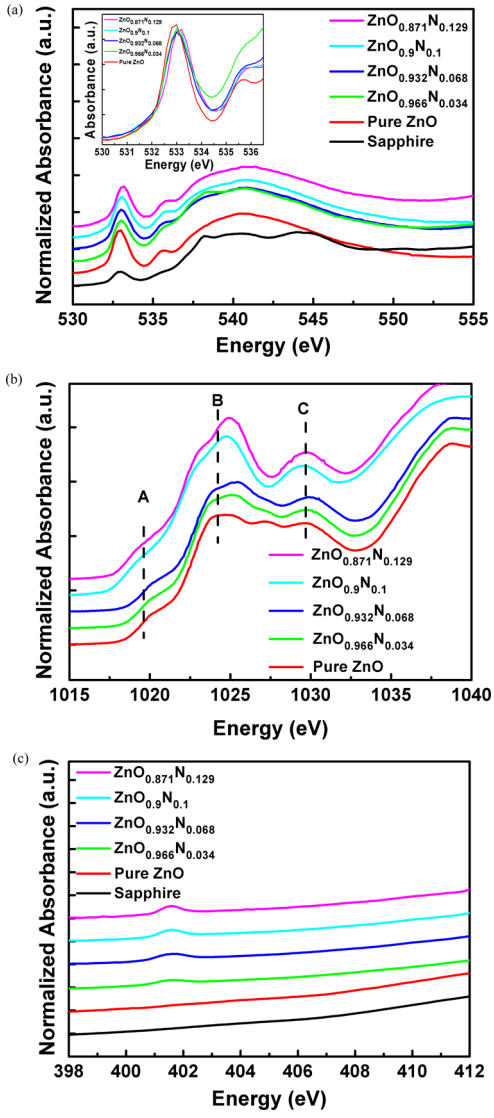

Figure 3. Normalized XANES spectra of the ZnO and ZnO:N thin films. (a) O *K*-edge and the insert shows a partial enlarged view of O *K*-edge, (b)Zn L_{III}-edge, and (c) N *K*-edge.

structure of oxygen atom is influenced sensitively by the content of N species. Therefore, the spectral variation of XANES at O *K*-edge with the N content can directly provide useful structural information about the electronic structure of the oxygen ion and the bonding character with Zn metal ion. In comparison with the first-principles multiscattering simulation, the energy region between 530 and 550 eV is contributed to the electron transition from the oxygen 1s state to the oxygen 2p level.[35] In the photon energy range of ~530−539 eV, XAS can be mainly assigned to the O 2p hybridized with Zn *4s* states. The spectrum between 539 and 550 eV is mainly ascribed to the O 2p hybridized with Zn 4p states.[36] As we can see in the inset in Figure 3a, the intensity of the peak at ~533 eV decreases a little bit and its photon energy slightly shifts to higher energy with an increase of the N content, which might be caused by the replacement of O sites by N. The result also indicates a decrease in strength of the O 2p hybridized with Zn 4s states and a widening of the bandgap energy.[35] Figure 4

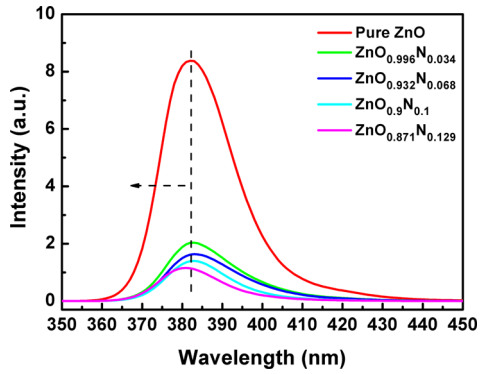

Figure 4. Room-temperature PL spectra of the pure ZnO and ZnO:N thin films.

shows the room-temperature PL spectra of the pure ZnO and ZnO:N films with various N contents. The PL spectral peak around 382 nm of the pure ZnO film can be identified as the near band-edge emission. A blue shift of the PL spectra was observed as the N content increased, which is in good agreement with the shift toward higher energy of the XAS peak at ~533 eV as shown in Figure 3a.

Figure 3b presents the Zn L_{III}-edge XAS spectra of the pure ZnO and ZnO:N thin films, revealing a spectral variation between 1015 to 1035 eV with an increase of the N content. The photon energy region is associated with the electron transitions from Zn 2p level to Zn 4s and antibonding 3d states.[37,38] It can be clearly seen in Figure 3b that the feature of peak B and C changes remarkably as the N content increases. Because the Zn 3d orbital is more localized than the Zn 4s orbital, the transition probability of Zn 2p to 3d could be greater than that of Zn 2p to 4s, and so the peak A is less sensitive. The shift of peak B and C toward higher energy indicates the increase in the energy of the valence state of Zn species, suggesting that the strength of the electron in Zn species caught by the O ligand gradually increases with an increase of the N content.[27] The result may be ascribed to the stronger electronegativity of oxygen than nitrogen as N and O bond with the Zn atom together, also implying the substitution of N for O sites. Figure 3c shows the N 1s absorption spectra of the pure ZnO and ZnO:N films. The clear N 1s absorption edge peak emerges at ~401.5 eV, which is consistent with the results of ZnO:N films reported by Jirsak and De Louise et

al.,[36,39] but different from that of the original N 1s, which is approximately located at 398 eV.[36] The shift in absorption energy could be a result of the incorporation of nitrogen in ZnO films.

Figure 5 displays the electron concentration and mobility of the ZnO:N thin films as a function of the N content. The

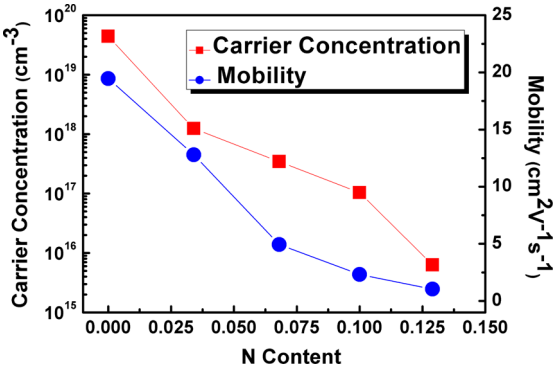

Figure 5. Electron concentration and mobility of the pure ZnO and ZnO:N thin films.

electron concentration decreases almost 4 orders of magnitude, from 1×10^{19} to 1×10^{15} cm^{-3}, with an increase of the N content from 0 to 0.129. Such significant decrease in the electron concentration can be attributed to the following mechanisms: (1) The incorporation of nitrogen into ZnO via the in situ atomic layer doping process may result in the formation of the N-related acceptors (N_o). Thus the decrease in electron concentration is due to the compensation of the intrinsic donor states by the N-related acceptors. (2) Because oxygen vacancies in ZnO were considered as the source of unintentional *n*-type conductivity, it is generally believed that oxygen vacancies act as donor states in ZnO.[40] Oxygen atmosphere in the post-RTA treatment may reduce the density of oxygen vacancies, resulting in the decrease of electron concentration. Accordingly the electron concentration decreases with the nitrogen incorporation and the RTA treatment in oxygen ambient. It is also seen that the electron mobility decreases from 19.46 cm^2 V^{-1} s^{-1} for the pure ZnO to 1.03 cm^2 V^{-1} s^{-1} for the $ZnO_{0.871}N_{0.129}$ film. The nitrogen in ZnO may act as the impurity scattering centers, which are responsible for the reduction in electron mobility.[41,42] Therefore, the electrical properties of ZnO:N films characterized by the Hall effect measurement are correspondent with the substitution of N for O in the ZnO:N films, as indicated by the XPS and XANES measurements.

CONCLUSIONS

In summary, the remote plasma in situ atomic layer doping technique was used to prepare ZnO:N thin films. The N content in the ZnO:N films exhibits a linear dependence on the nitrogen atomic layer doping percentage, indicating that the N content can be precisely controlled by the number of atomic doped layers and their separation in the films. Heavily doped ZnO:N thin films with the N content as high as 12.9% can be achieved using this in situ atomic layer doping technique. XPS, XAS and Hall effect measurements were performed to investigate the correlation between the local electronic structures and the electrical properties of the ZnO:N thin films. The XPS spectrum indicates the formation of the Zn−N bond and the N content in the ZnO:N films was identified by the XPS analysis. The XANES measurement presents a decrease in strength of the O 2p hybridized with Zn 4s states and an increase in the valence state energy of Zn species, as results of the substitution of N for O sites. The O *K*-edge XANES spectra also reveals an increase of the bandgap energy, which agrees well with the blue shift in the PL spectra. The Hall effect measurement shows a significant decrease of electron concentration in the ZnO:N films with an increase of the N content. This can be deduced from the formation of N-related acceptor states (N_o) by occupation of O sites with N species, which is consistent with the XPS and XANES measurements. The results indicate that the in situ atomic layer doping technique is an effective method for modifying the electrical characteristics of ZnO. The ZnO:N thin films will be applied in the ZnO-based devices for future studies.

AUTHOR INFORMATION

Corresponding Author

*E-mail: mjchen@ntu.edu.tw.

Notes

The authors declare no competing financial interest.

ACKNOWLEDGMENTS

This work was financially supported by the National Science Council in Taiwan under contract number NSC 100-2120-M-002-014 and NSC 101-3113-E-002-009. The authors are grateful for the support of XANES measurement at the National Synchrotron Radiation Research Center in Hsinchu, Taiwan.

REFERENCES

(1) Huang, M. H.; Mao, S.; Feick, H.; Yan, H. Q.; Wu, Y. Y.; King, H.; Weber, E.; Russo, R.; Yang, P. *Science* **2001**, *292*, 1897.
(2) Rogers, D. J.; Hosseini Teherani, F.; Yasan, A.; Minder, K.; Kung, P.; Razeghi, M. *Appl. Phys. Lett.* **2006**, *88*, 141918.
(3) Guo, X. L.; Choi, J. H.; Tabata, H.; Kawai, T. *Jpn. J. Appl. Phys. Lett.* **2001**, *40*, L177−L188.
(4) Lim, S. J.; Kim, J. M.; Kim, D.; Kwon, S.; Park, J. S.; Kimb, H. *J. Electrochem. Soc.* **2010**, *157*, H214.
(5) Kwon, S.; Bang, S.; Lee, S.; Jeon, S.; Jeong, W.; Kim, H.; Gong, S. C.; Chang, H. J.; Park, H. H.; Jeon, H. *Semicond. Sci. Technol.* **2009**, *24*, 035015.
(6) Chen, H. C.; Chen, M. J.; Liu, T. C.; Yang, J. R.; Shiojiri, M. *Thin Solid Films* **2010**, *519*, 536.
(7) Look, D. C.; Hemsky, J. W.; Sizelove, J. R. *Phys. Rev. Lett.* **1999**, *82*, 2552.
(8) Wenckstern, H. V.; Benndorf, G.; Heitsch, S.; Sann, J.; Brandt, M.; Schmidt, H.; Lenzner, J.; Lorenz, M.; kuznetsov, A. Y.; Meyer, B. K.; Grundmann, M. *Appl. Phys. A: Mater. Sci. Process.* **2007**, *88*, 125.
(9) Ryu, Y. R.; Lee, T. S.; White, H. W. *Appl. Phys. Lett.* **2003**, *83*, 87.
(10) Park, C. H.; Zhang, S. B.; Wei, S. H. *Phys. Rev. B* **2002**, *66*, 073202.
(11) Tsukazaki, A.; Ohtomo, A.; Onuma, T.; Ohtani, M.; Makino, T.; Sumiya, M.; Ohtani, K.; Chichibu, S. F.; Fuke, S.; Segawa, Y.; Ohno, H.; Koinuma, H.; Kawasaki, M. *Nat. Mater.* **2005**, *4*, 42.
(12) Sun, J. C.; Liang, H. W.; Zhao, J. Z.; Bian, J. M.; Feng, Q. J.; Hu, L. Z.; Zhang, H. Q.; Lianga, X. P.; Luoa, Y. M.; Dua, G. T. *Chem. Phys. Lett.* **2008**, *460*, 548.
(13) Lim, S. J.; Kwon, S. J.; Kim, H.; Park, J. S. *Appl. Phys. Lett.* **2007**, *91*, 183517.
(14) Hsieh, H. H.; Wu, C. C. *Appl. Phys. Lett.* **2007**, *91*, 013502.
(15) Martins, R.; Barquinha, P.; Ferreira, I.; Pereira, L.; Gonçalves, G.; Fortunato, E. *J. Appl. Phys.* **2007**, *101*, 044505.
(16) Tan, S. T.; Chen, B. J.; Sun, X. W.; Fan, W. J. *J. Appl. Phys.* **2005**, *98*, 013505.

(17) Anderson, P. W. *Phys. Rev.* **1985**, *109*, 1492.
(18) Liu, Y.; Gorla, C. R.; Liang, S.; Emanetoglu, N.; Lu, Y.; Shen, H.; Wraback, M. *J. Electron. Mater.* **2000**, *29*, 70.
(19) Liu, W.; Gu, S. L.; Ye, J. D.; Zhu, S. M.; Liu, S. M.; Zhou, X.; Zhang, R.; Shi, Y.; Zheng, Y. D. *Appl. Phys. Lett.* **2006**, *88*, 092101.
(20) Jiao, S. J.; Zhang, Z. Z.; Lu, Y. M.; Shen, D. Z.; Yao, B.; Zhang, J. Y.; Li, B. H.; Zhao, D. X.; Fan, X. W.; Tang, Z. K. *Appl. Phys. Lett.* **2006**, *88*, 031911.
(21) Epurescu, G.; Dinescu, G.; Moldovan, A.; Birjega, R.; Dipietrantonio, F.; Verona, E.; Verardi, P.; Nistor, L. C.; Ghica, C.; Van Tendelood, G.; Dinescua, M. *Superlattices Microstruct.* **2007**, *42*, 79.
(22) Kim, H.; Cepler, A.; Cetina, C.; Knies, D.; Osofsky, M. S.; Auyeung, R. C. Y.; Piqué, A. *Appl. Phys. A: Mater. Sci. Process.* **2008**, *93*, 593.
(23) Singh, A. V.; Mehra, R. M.; Wakahara, A.; Yoshida, A. *J. Appl. Phys.* **2003**, *93*, 396.
(24) Chen, L. L.; Lu, J. G.; Ye, Z. Z.; Lin, Y. M.; Zhao, B. H.; Ye, Y. M.; Li, J. S.; Zhu, L. P. *Appl. Phys. Lett.* **2005**, *87*, 252106.
(25) Niinistö, L.; Päiväsaari, J.; Niinistö, J.; Putkonen, M.; Nieminen, M. *Phys. Status Solidi A* **2004**, *201*, 1443.
(26) Lim, J.; Shin, K.; Kim, H. W.; Lee, C. *J. Lumin.* **2004**, *109*, 181.
(27) Guziewicz, E.; Kowalik, I. A.; Godlewski, M.; Kopalko, K.; Osinniy, V.; Wójcik, A.; Yatsunenko, S.; Usakowska, E.; Paszkowicz, W.; Guziewicz, M. *J. Appl. Phys.* **2008**, *103*, 033515−1.
(28) Chen, H. C.; Chen, M. J.; Wu, M. K.; Cheng, Y. C.; Tsai, F. Y. *IEEE J. Sel. Topics Quantum Electron* **2008**, *14*, 1053.
(29) Scappucci, G.; Capellini, G.; Klesse, W. M.; Simmons, M. Y. *Nanotechnology* **2011**, *22*, 375203.
(30) Waychunas, G. A.; Fuller, C. C.; Davis, J. A.; Rehr, J. J. *Geochim. Cosmochim. Acta* **2003**, *67*, 1031.
(31) Bencze, K. Z.; Kondapalli, K. C.; Stemmler, T. L. *Encyclopedia of Inorganic Chemistry*; John Wiley & Sons: New York, 2008.
(32) Cruz-Vázquez, C.; Rocha-Alonzo, F.; Burruel-Ibarra, S. E.; Inoue, M. *Superficies Vacío* **2001**, *13*, 89.
(33) Toumiat, A.; Zerkout, S.; Achour, S.; Tabet, N.; Guarbous, L. *Am. Inst. Physi. Conf. Proc.* **2007**, *929*, 59.
(34) Joseph, M.; Tabata, H.; Saeki, H.; Ueda, K.; Kawai, T. *Physica B* **2001**, *302*−*303*, 140.
(35) Chiou, J. W.; Kumar, K. P.; Jan, J. C.; Tsai, H. M.; Bao, C. W.; Pong, W. F.; Chien, F. Z. *Appl. Phys. Lett.* **2004**, *85*, 3220.
(36) Jirsak, T.; Dvorak, J.; Rodriguez, J. A. *Surf. Sci.* **1999**, *436*, L683.
(37) Mizoguchia, T.; Yoshiyaa, M.; Lia, J.; Obaa, F.; Tanakab, I.; Adachia, H. *Ultramicroscopy* **2001**, *86*, 363.
(38) Cho, D. Y.; Kim, J. H.; Na, K. D.; Song, J.; Hwang, C. S.; Park, B. G.; Kim, J. Y.; Min, C. H.; Oh, S. J. *Appl. Phys. Lett.* **2009**, *95*, 261903.
(39) Delouise, L. A.; Winograd, N. *Surf. Sci.* **1985**, *159*, 199.
(40) Singh, A. V.; Mehra, R. M.; Wakahara, A.; Yoshida, A. *J. Appl. Phys.* **2003**, *93*, 396.
(41) Lu, J.; Zhang, Y.; Ye, Z.; Wang, L.; Zhao, B.; Huang, J. *Mater. Lett.* **2003**, *57*, 3311.
(42) Lim, S. J.; Kwon, S.; Kim, H.; Park, J. S. *Appl. Phys. Lett.* **2007**, *91*, 183517.